Electronic Supplementary Material (ESI) for Journal of Materials Chemistry A.

Electronic Supplementary Information

Ethynyl-linked Fe/Co Heterometallic Phthalocyanine Conjugated Polymer for Oxygen Reduction Reaction

Wenping Liu,[a] Yuxia Hou,[a,c] Houhe Pan,[a] Wenbo Liu,[a] Dongdong Qi,*[a] Kang Wang,*[a,b]

Jianzhuang Jiang*[a] and Xiangdong Yao[b]

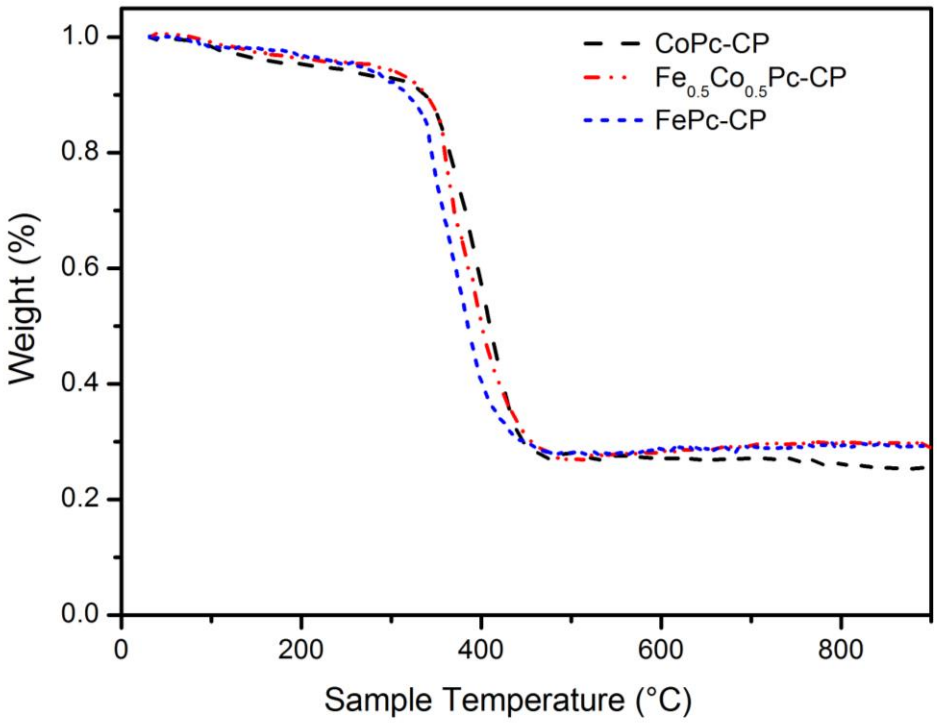

Fig. S1 TGA of **CoPc-CP**, **$Fe_{0.5}Co_{0.5}$Pc-CP**, and **FePc-CP**.

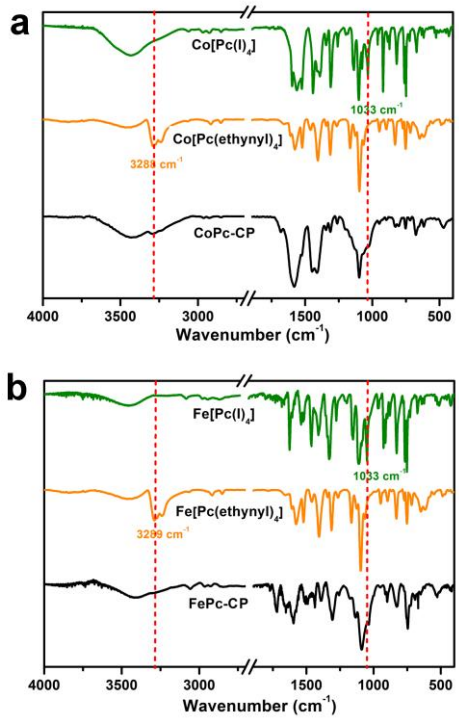

Fig. S2 FT-IR spectra of (a) **CoPc-CP** and (b) **FePc-CP** as well as the corresponding phthalocyanine monomers in the region of 400-4000 cm^{-1}.

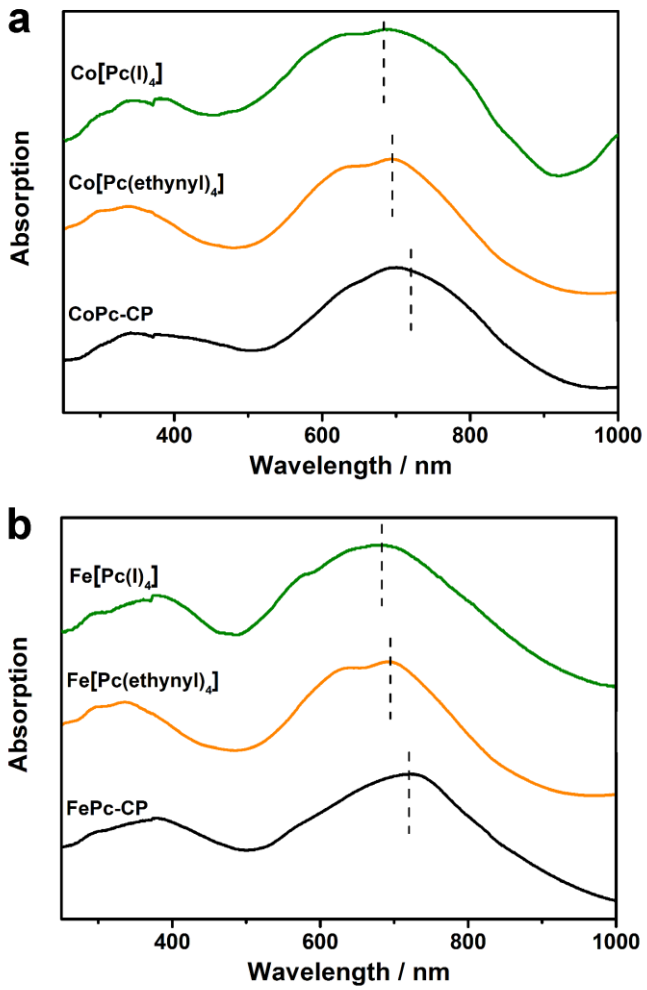

Fig. S3 UV-vis diffuse reflectance spectra of (a) **CoPc-CP** and (b) **FePc-CP** as well as the corresponding phthalocyanine monomers.

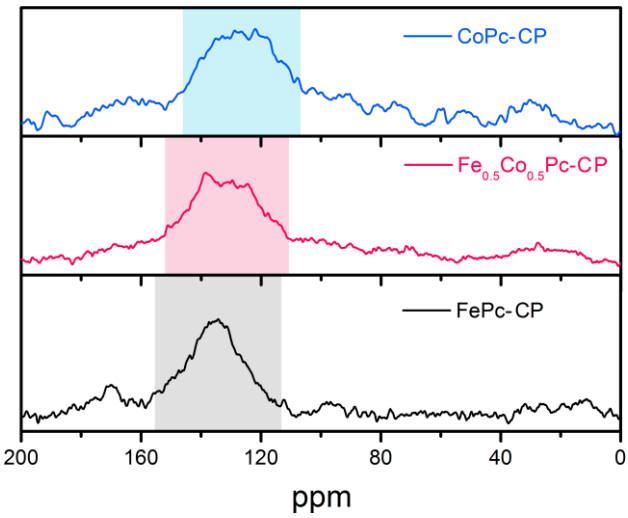

Fig. S4 ^{13}C CP/MAS NMR spectra of **CoPc-CP**, **$Fe_{0.5}Co_{0.5}$Pc-CP**, and **FePc-CP**.

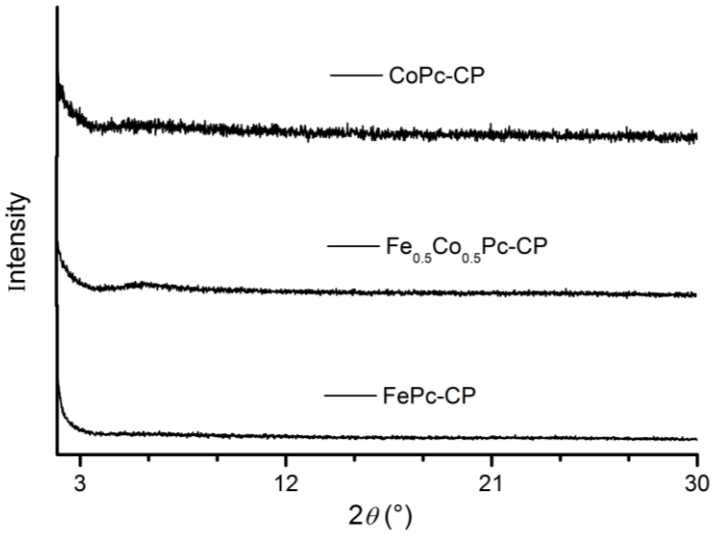

Fig. S5 PXRD patterns of **CoPc-CP**, **FePc-CP**, and **$Fe_{0.5}Co_{0.5}$Pc-CP**.

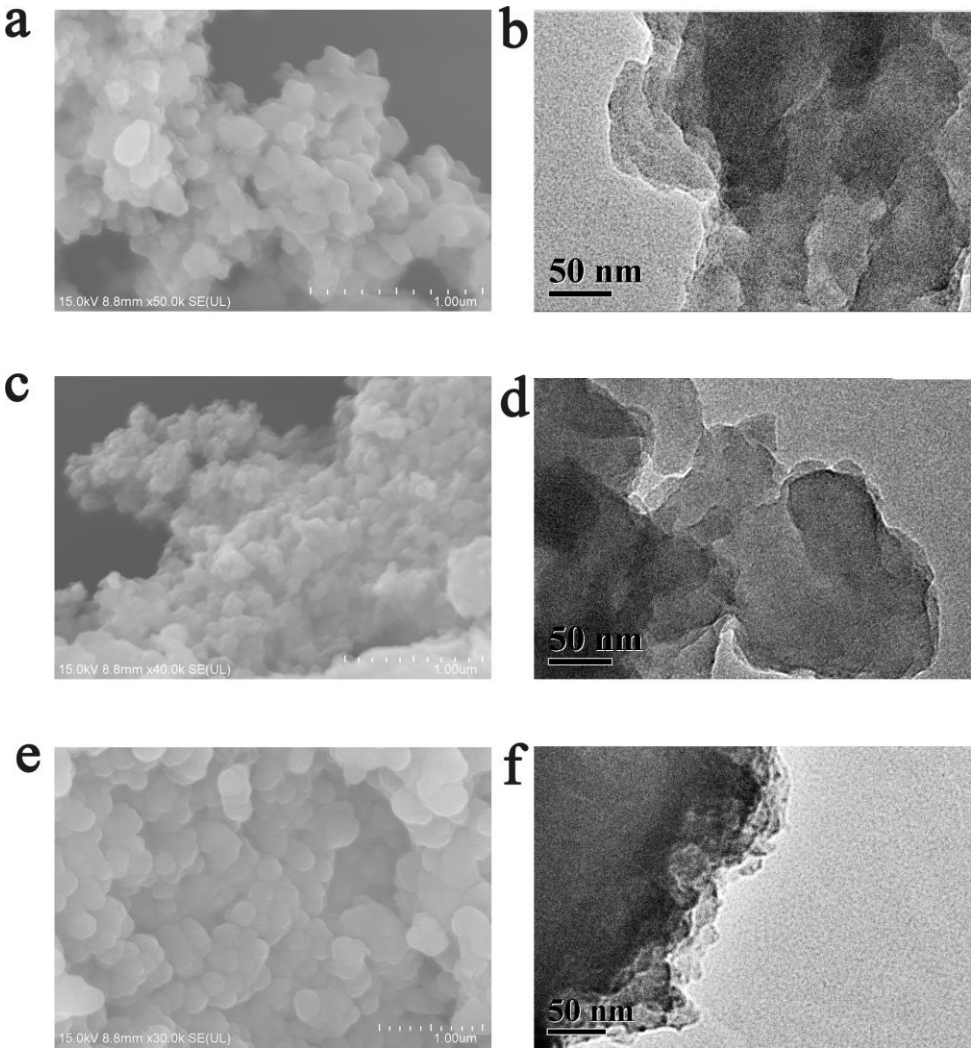

Fig. S6 SEM and TEM images of (a, b) **CoPc-CP**, (c, d) **$Fe_{0.5}Co_{0.5}$Pc-CP**, and (e, f) **FePc-CP**.

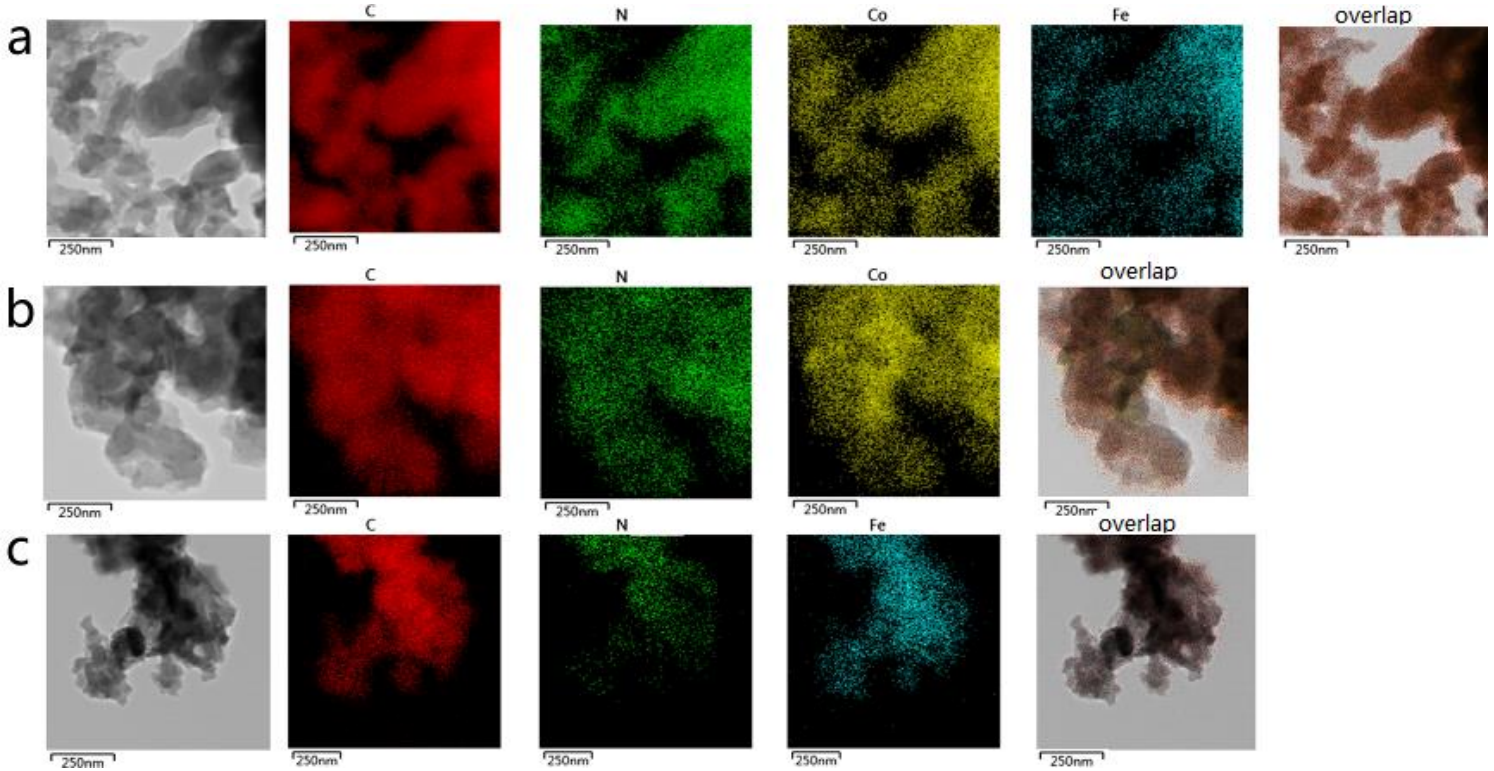

Fig. S7 The STEM and elemental-mapping images of (a) **$Fe_{0.5}Co_{0.5}$Pc-CP**, (b) **CoPc-CP**, and **(**c) **FePc-CP**.

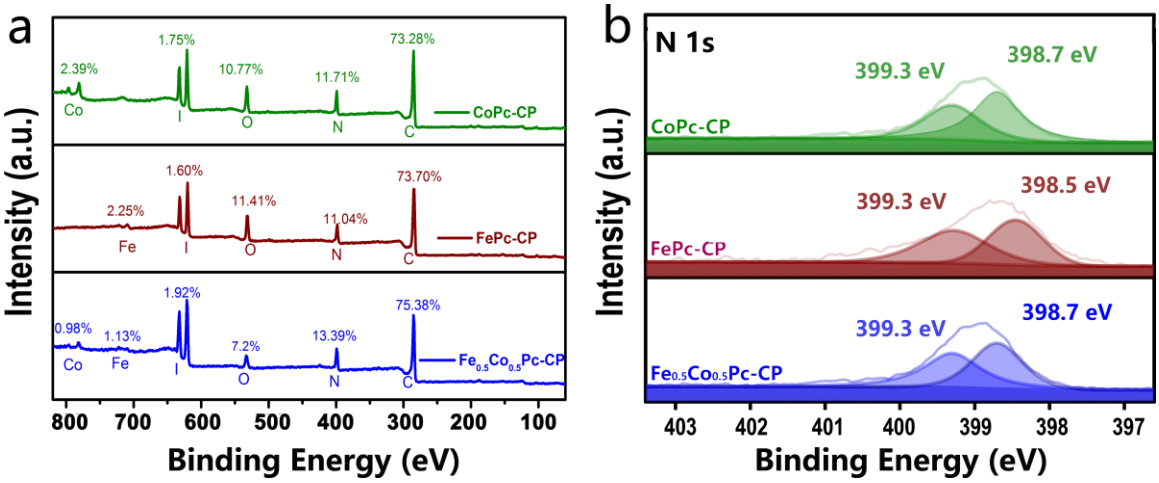

Fig. S8 XPS (a) overall spectra and (b) high resolution N 1s spectra of **CoPc-CP**, **FePc-CP**, and **$Fe_{0.5}Co_{0.5}$Pc-CP**.

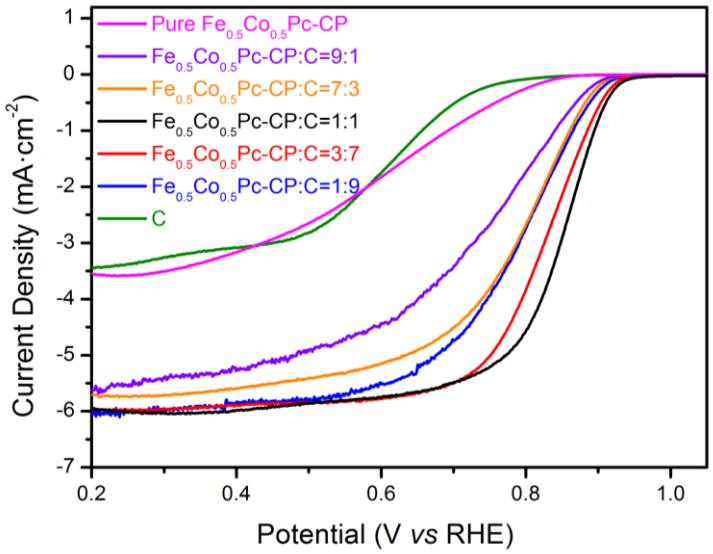

Fig. S9 LSV curves of pure XC-72 and **$Fe_{0.5}Co_{0.5}$Pc-CP&XC-72** mixture with different contents measured at the scan rate of 10 mV s^{-1} with the rotation speed of 1600 rpm in O_2-saturated 0.1 M KOH solution.

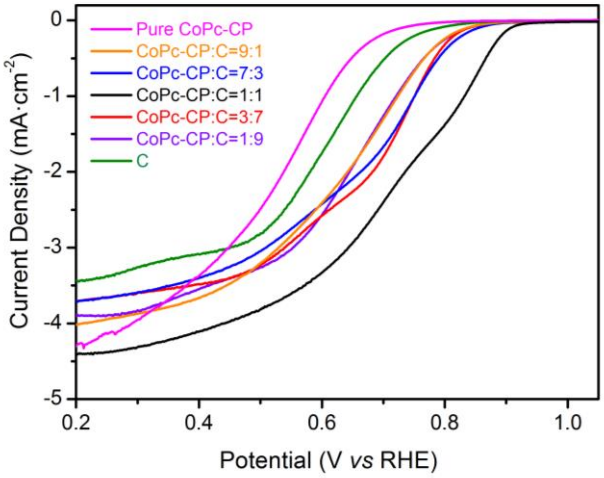

Fig. S10 LSV curves of pure XC-72 and **CoPc-CP&XC-72** mixture with different contents measured at the scan rate of 10 mV s^{-1} with the rotation speed of 1600 rpm in O_2-saturated 0.1 M KOH solution.

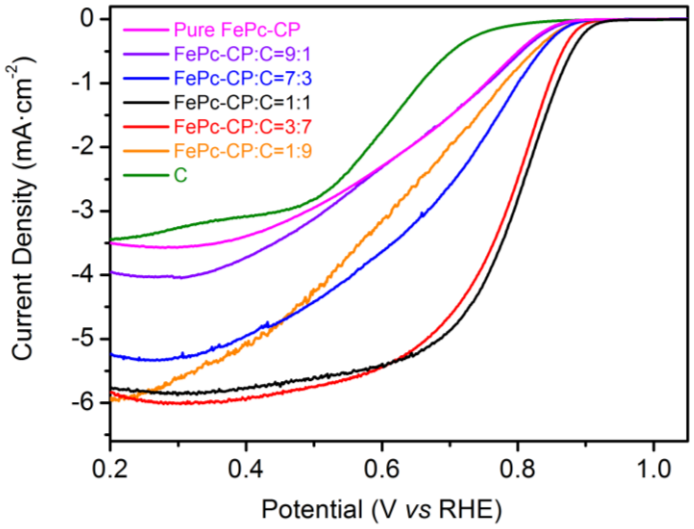

Fig. S11 LSV curves of pure XC-72 and **FePc-CP&XC-72** mixture with different contents measured at the scan rate of 10 mV s^{-1} with the rotation speed of 1600 rpm in O_2-saturated 0.1 M KOH solution.

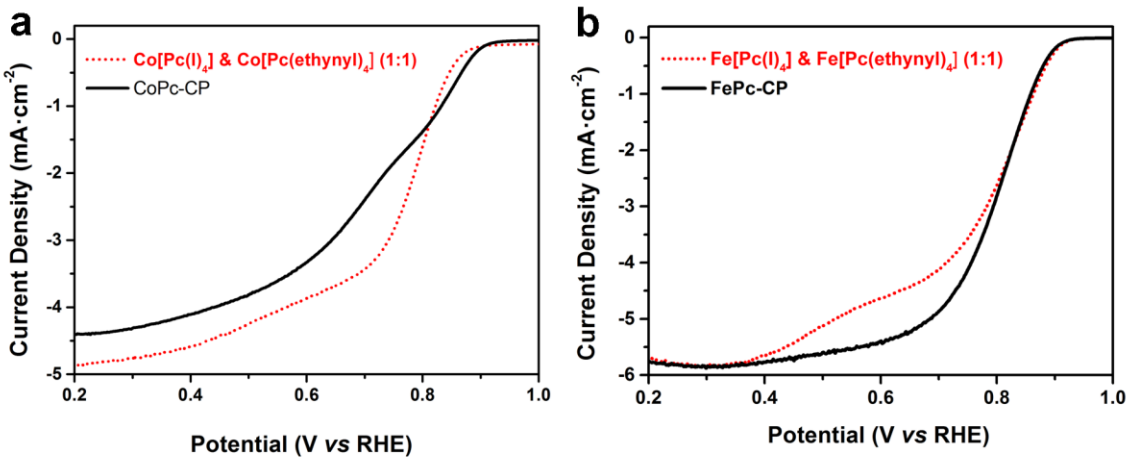

Fig. S12 LSV curves of (a) Co[Pc(I)$_4$] & Co[Pc(ethynyl)$_4$] (1:1) and **CoPc-CP** and (b) Fe[Pc(I)$_4$] & Fe[Pc(ethynyl)$_4$] (1:1) and **FePc-CP** at the scan rate of 10 mV s^{-1} with the rotation speed of 1600 rpm in O_2-saturated 0.1 M KOH solution. All the date were measured by doping with 50 wt% XC-72.

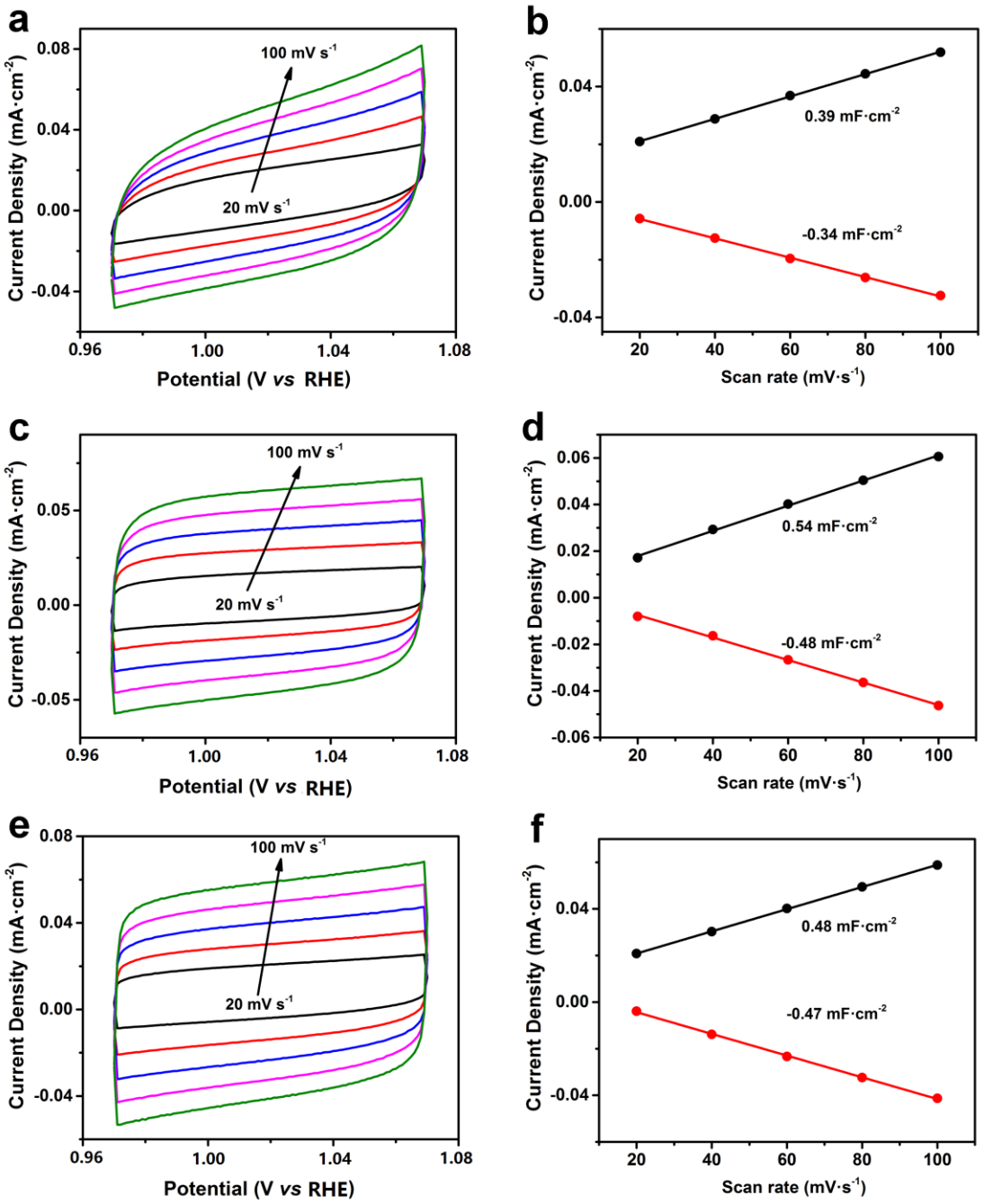

Fig. S13 (a)(c)(e) CV conducted at potential from 0.97 V to 1.07 V *vs* RHE at scan rates of 20 mV s^{-1}, 40 mV s^{-1}, 60 mV s^{-1}, 80 mV s^{-1}, and 100 mV s^{-1} in 0.1 M KOH. (b)(d)(f) The current densities of anode and cathode measured at 1.02 V *vs* RHE with different scan rates. (a)(b), (c)(d) and (e)(f) are **CoPc-CP** with 50 wt% XC-72, **FePc-CP** with 50 wt% XC-72, and **$Fe_{0.5}Co_{0.5}$Pc-CP** with 50 wt% XC-72, respectively.

To study the electrochemically active surface area (ECSA) of **CoPc-CP** with 50 wt% XC-72, **FePc-CP** with 50 wt% XC-72, and **$Fe_{0.5}Co_{0.5}$Pc-CP** with 50 wt% XC-72, we conducted the CV cycles at different scan rates during the potential from 0.97 V to 1.07 V *vs* RHE in 0.1 M KOH, where there is no Faradic current. At last, the ECSA was estimated from the as obtained double-layer capacitance (C_{dl}). According to C_{dl} is constant, it can be calculated as:

$$C_{dl} = Q/U = (dQ/dt)/(dU/dt) = j/r \quad (1)$$

Q is the quantity of electric charge per unit area,

U is the voltage,

j is the current density and

r is the scan rate.

From Eq(1), the C_{dl} is the slope of *j*~*r*, which can be obtained by the Figure S13b, d and f. The average C_{dl} of **CoPc-CP** with 50 wt% XC-72, **FePc-CP** with 50 wt% XC-72, and **$Fe_{0.5}Co_{0.5}$Pc-CP** with 50 wt% XC-72 are 0.36 mF/cm^2, 0.51 mF/cm^2, and 0.48 mF/cm^2, respectively. The ECSA can be calculated as:

$$ECSA = C_{dl}/C_s \quad (2)$$

C_s is the specific capacitance value for a flat standard with 1 cm^2 of real surface area. The general value for C_s is between 20 μF/cm^2 and 60 μF/cm^2. Here we use 40 μF/cm^2 as the average value (*Nat. Commun.* **2015**, *6*, 8668). Thus the ECSA for **CoPc-CP** with 50 wt% XC-72, **FePc-CP** with 50 wt% XC-72, and **$Fe_{0.5}Co_{0.5}$Pc-CP** with 50 wt% XC-72 can be obtained as 9.0 cm^2, 13 cm^2, and 12 cm^2, respectively.

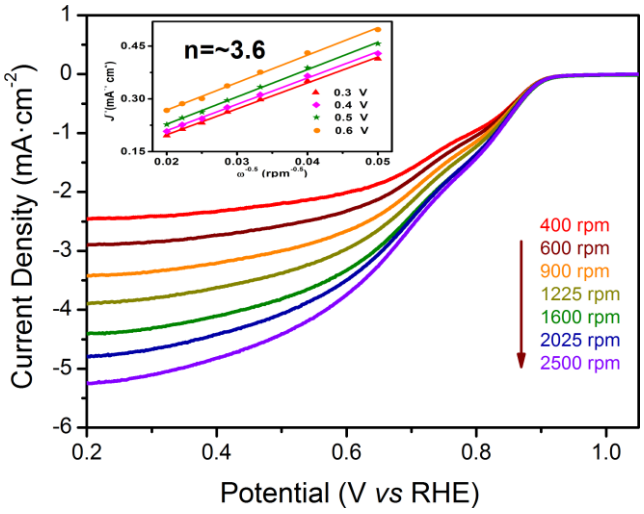

Fig. S14 LSV curves of **CoPc-CP**-loaded electrode with loading amount of 50 wt% at different rotation speeds with the scan rate of 10 mV s^{-1} in O_2-saturated 0.1 M KOH solution, Insert: Koutecky–Levich (K–L) plots at different potentials.

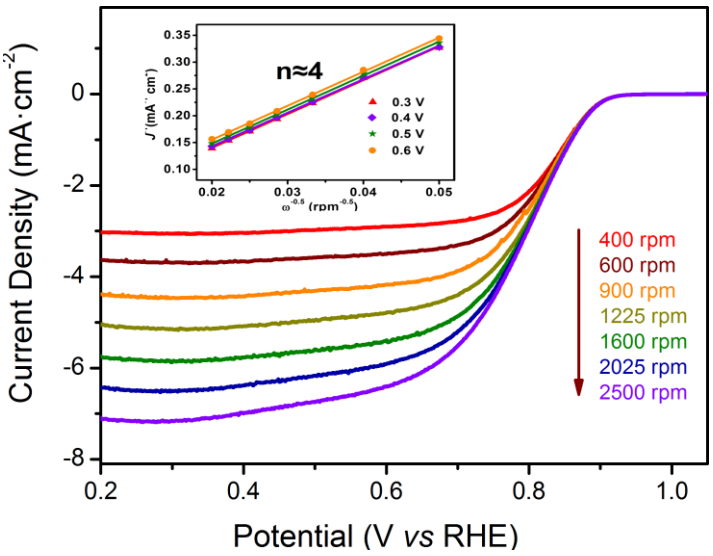

Fig. S15 LSV curves of **FePc-CP**-loaded electrode with loading amount of 50 wt% at different rotation speeds with the scan rate of 10 mV s^{-1} in O_2-saturated 0.1 M KOH solution, Insert: Koutecky–Levich (K–L) plots at different potentials.

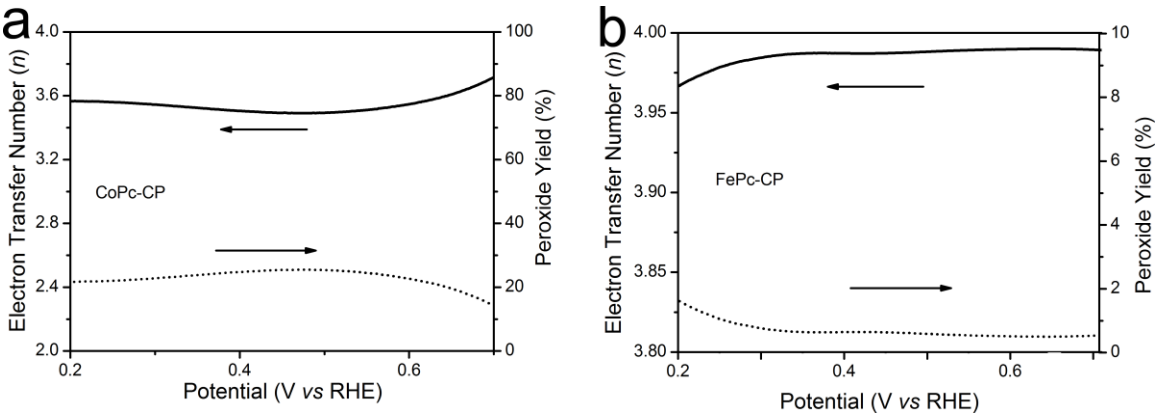

Fig. S16 Percentage of peroxide species (dotted solid lines) and the electron-transfer number (n) (solid lines) of (a) **CoPc-CP**- and (b) **FePc-CP**-loaded electrode with 50 wt% XC-72 in the potential range of 0.20-0.70 V (calculated from the corresponding RRDE data).

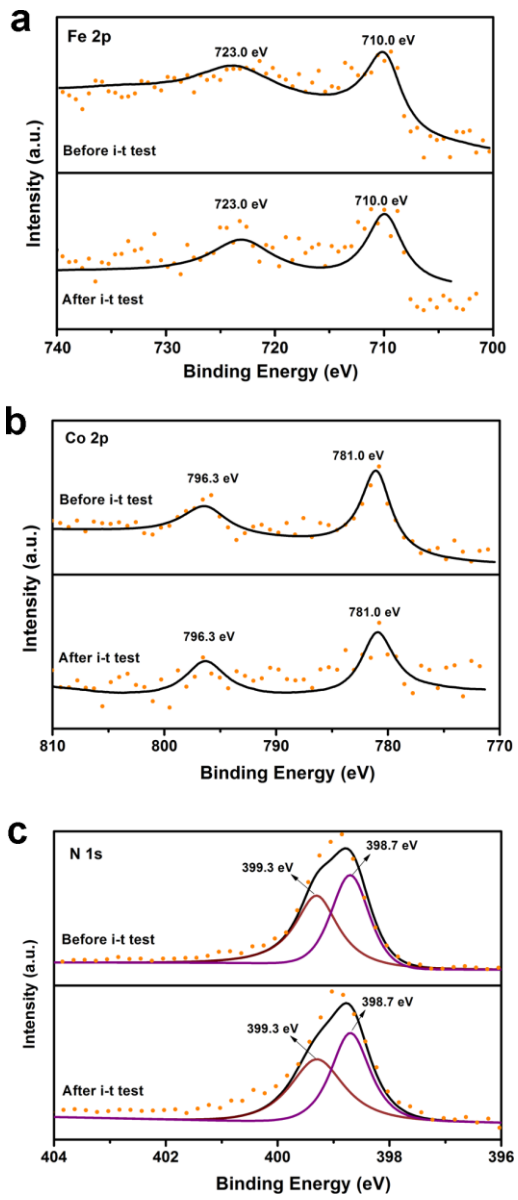

Fig. S17 XPS high resolution (a) Fe 2p, (b) Co 2p, and (c) N 1s spectra of **$Fe_{0.5}Co_{0.5}$Pc-CP** before and after i-t test.

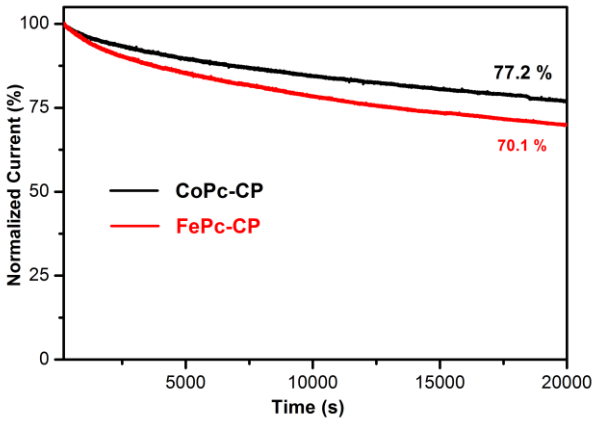

Fig. S18 Amperometric i–t curves of **CoPc-CP** and **FePc-CP**-modified electrode tested with the rotation speed of 1600 rpm in O_2-saturated 0.1 M KOH solution.

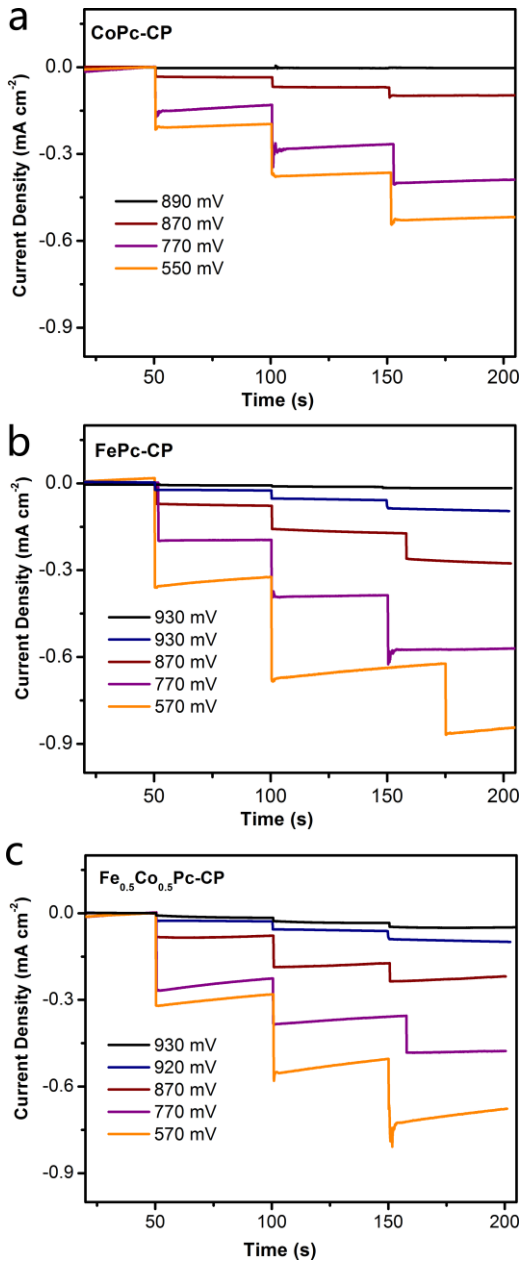

Fig. S19 Current−time (I−t) curves of **CoPc-CP**, **FePc-CP**, and **$Fe_{0.5}Co_{0.5}$Pc-CP** electrode in the potential range of 570 and 930 mV with successive injection of 1 mM H_2O_2 into N_2-saturated 0.1 M KOH solution.

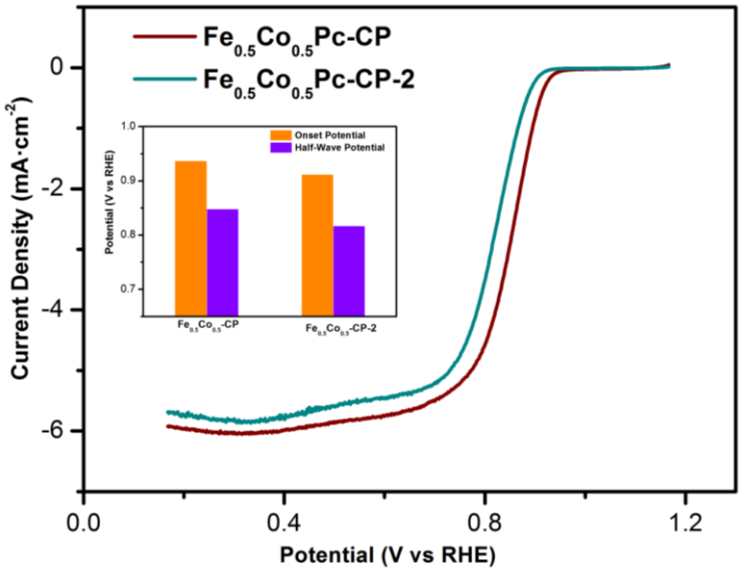

Fig. S20 LSV curves of **$Fe_{0.5}Co_{0.5}$Pc-CP** and **$Fe_{0.5}Co_{0.5}$Pc-CP-2-**modified electrode tested with the rotation speed of 1600 rpm in O_2-saturated 0.1 M KOH solution. Inset: Half-wave potential and onset potential comparisons of **$Fe_{0.5}Co_{0.5}$Pc-CP** and **$Fe_{0.5}Co_{0.5}$Pc-CP-2**.

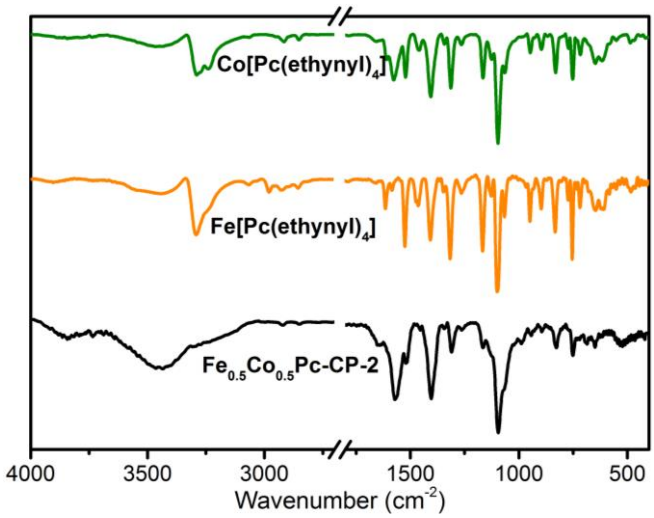

Fig. S21 FT-IR spectra of **$Fe_{0.5}Co_{0.5}$Pc-CP-2** as well as the corresponding phthalocyanine monomers in the region of 400-4000 cm^{-1}.

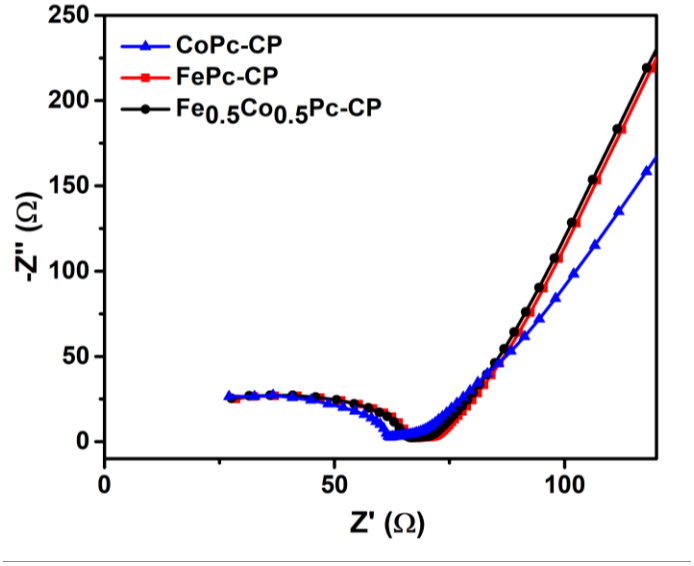

Fig. S22 Impedance curve of **CoPc-CP**, **FePc-CP**, and **$Fe_{0.5}Co_{0.5}$Pc-CP** with 50 wt% XC-72.

Table S1. Summary of the electrochemical properties for the ORR catalysts.

Sample	Catalyst loading [mg cm^{-2}]	E_{onset}[a] [mV]	$E_{1/2}$[b] [mV]	$\|J_L\|$[c] [mA cm^{-2}]	n[d]
CoPc-CP	0.08	907	716	4.40	3.49
FePc-CP	0.08	910	800	5.76	3.98
$Fe_{0.5}Co_{0.5}$Pc-CP	0.08	937	848	5.98	3.97
Pt/C	0.08	951	823	6.14	3.96

[a] Onset potential was acquired at an ORR current density of 0.1 mA cm^{-2} in a steady-state RDE experiment; [b] Half-wave potential; [c] Limiting current density was obtained at 0.2 V (vs RHE) with the rotation speed of 1600 rpm; [d] Electron transfer number was calculated at 0.5 V (vs RHE) from the corresponding RRDE data.